Jurnal rekayasa mesin
Vol. 17. No.1
ISSN 2477-6041 articles 4, pp. 33 – 44, 2026

VALIDATION OF EXPERIMENTAL STUDY AND SIMULATION OTEC POWER PLANT USING SHELL-TUBE HEAT EXCHANGER MATERIALS WITH COPPER, TIN, AND WORKING FLUID AMMONIA

Mawardi[1)]✉, Zufri Hasrudy Siregar[1)], Yoga Tri Nugraha[2)], Rizkha Rida[3)], Tengku M Fahri[4)], Muhammad Irwanto[5)]

[1)] **Department of Mechanical Engineering**
Lecturer of the Faculty of Engineering,
Universitas Al-Azhar Pintu Air IV. No. 214
Kwala Bekala, Padang Bulan Medan,
Sumatra Utara, INDONESIA
mawardi.ipc@gmail.com
rudysiregar7@gmail.com

[2)] **Department of Electrical Engineering**
Lecturer of the Faculty of Engineering,
Universitas Al-Azhar Pintu Air IV. No. 214
Kwala Bekala, Padang Bulan Medan,
Sumatra Utara, INDONESIA
yogatrinugraha16@gmail.com

[3)] **Industrial Engineering Department**
Lecturer of the Faculty of Engineering,
Universitas Al-Azhar Pintu Air IV. No. 214
Kwala Bekala, Padang Bulan Medan,
Sumatra Utara, INDONESIA
rizkharida26@gmail.com

[4)] **Civil Engineering Department**
Lecturer of the Faculty of Engineering,
Universitas Al-Azhar Pintu Air IV. No. 214
Kwala Bekala, Padang Bulan Medan,
Sumatra Utara, INDONESIA
tengku.muhammad.fahri@gmail.com

[5)] **Department of Electrical Engineering**
Lecturer of the Faculty of Engineering,
Universitas Prima Indonesia Jl. Sampul.
No. 3 Medan Petisah, INDONESIA

Abstract

The results of experimental research on marine thermal power plants using a shell and tube heat exchanger made of copper-tin (Cu-Sn) alloy are the main focus of this study. This study uses a heat exchanger Scale Model measuring 60 mm wide x 1 meter long. The system operated using a closed cycle and Organic Rankin cycle. A simulation study has been carried out using Ansys CFD software to model new heat exchangers, namely models A and B. The interaction between ammonia and hot water produces thermodynamic values in the form of an evaporator outlet temperature of 28°C in models A and B 260C. The weakness of model B is that the turbulent flow is divided into left and right sides so that heat loss occurs in the flow corner area. The seawater inlet temperature of 29°C can heat the working fluid from the ammonia flow inlet from 5°C to 28°C, resulting in saturated steam reaching 5-6 bar.

Keywords: *OTEC, Heat Exchanger, Shell and Tube, Ammonia, Copper-Tin.*

Corresponding Author:
✉ **Mawardi**
Received on : 2025-01-26
Revised on : 2026-01-18
Accepted on : 2026-03-16

1. INTRODUCTION

Indonesia's enormous renewable energy potential remains untapped, one of which is OTEC Ocean energy [1] . Ocean thermal energy power generation (OTEC) is generated through the temperature difference between warm water at the sea surface (290 °C) and water at 50 °C 1000 meters inland [2]. One of the OTEC plants is operated using the Rankine cycle with ammonia as the working fluid, where the seawater outlet from the condenser in the closed organic Rankine cycle is used to provide the cooling medium [3]. As part of renewable technology, OTEC produces a clean energy source; the working fluid ammonia in the evaporator in a closed cycle is not released or flowed into the environment, so it does not cause environmental pollution [4]. The selection of an

DOI: 10.21776/jrm.v17i1.2049

appropriate heat exchanger type based on temperature range and cost is a critical factor in industrial applications [5]. The OTEC plant with a titanium plate-type Heat Exchanger (PHE) has excellent corrosion resistance, but the cost factor of this material means that research into OTEC energy must consider alternatives to replace other anti-corrosion heat exchanger materials [6]. Given these conditions, we conducted this research using a tin-copper (Cu-Sn) alloy heat exchanger. It's more economical than titanium and readily available on the market. To produce the desired saturated steam, the shell-and-tube heat exchanger system uses ammonia as the working fluid, which powers the turbine [7]. OTEC is a power generator that uses the temperature difference in seawater as a realistic heat source with limited heat capacity; its temperature will change continuously from time to time during the heat transfer process in the evaporator [8]. This research aims to generate power using the work produced by the evaporator in a closed-cycle system that utilizes the temperature difference between surface seawater and deep seawater. Additionally, other studies have explored the use of solar energy to further increase seawater temperature in the Kalina combined cycle OTEC (Ocean Thermal Energy Conversion) system. Power output is evaluated using the Aspen Plus simulation, with turbine inlet pressures exceeding 2.9 MPa and turbine outlet pressures ranging between 1.3 and 1.6 MPa [9]. Based on the references discussed above, the researcher intends to replace the titanium corrosion-resistant heat exchanger with a more affordable and economical copper-tin alloy. A shell-and-tube heat exchanger was selected to minimize power losses associated with turbulence, which frequently occurs in plate-type heat exchangers.

2. LITERATURE REVIEW AND PROBLEM FORMULATION

This journal [3] developed research on the analysis of three Ocean Thermal Energy Converter (OTEC)-based models or systems using the Aspen Plus simulation model approach at 1 bar pressure, where ammonia is operated as the working fluid, variations in the cooling water flow rate, and power. The highest efficiency value of the cycle is found in the amount of heat absorbed the most because it has the highest working fluid flow rate. Resulting in maximum energy and exergy efficiency of the OTEC plant of 1.83% and 78.02%, and 1.37% and 56.17%, respectively. The research study in this paper [10] Discusses and examines gaps in current economic analysis, the impact of outputs such as net power, component costs, budget expenditures, or operational costs, and the impact on society in the form of interest rates and electricity operational costs in the OTEC industrial system. However, its weakness is that it does not yet consider Break-Even Point (BEP) costs. This research paper's findings study [11] This paper discusses an irreversible regenerative organic Rankine cycle model based on finite-time thermodynamics. It analyzes the effect of internal irreversible losses on the power output and thermal efficiency of this cycle. The study reveals that this paper requires attention, as internal power losses cannot be changed, significantly affecting the resulting power output.

I've proposed edits to clarify and improve the flow of your paragraph, emphasizing the unavoidable nature of internal power losses and their impact on the cycle's performance. Analysis of this Journal [12] Discussing the advantages of titanium flat-plate heat exchangers for OTEC plants due to their corrosion resistance. Titanium is a heating or cooling source for working fluids, making it a very suitable plate material at PHE due to its excellent corrosion resistance to seawater. However, the downside in our environment is the high cost factor, which means that very few energy enthusiasts are turning to this OTEC business.

The problem formulation that can be taken from this research is based on the results of the research and considering that the source of this OTEC system is seawater which is very susceptible to corrosive hazards but must also be in accordance with the political and economic conditions of this country, then copper tin (Cu-Sn) is very suitable as an alternative to titanium which is very capable of corrosion. The suitable model is also taken as a shell and tube compared to the flat plate model because it avoids the occurrence of saturated steam loss that occurs during production.

3. RESEARCH PURPOSES

This research study is entitled " Validation of Experimental Research Results and advanced simulation of Ocean Thermal Conversion Power Plants (OTEC) using a shell and tube heat exchanger model made of copper-tin alloy and ammonia as the fluid. This research was conducted with the aim of obtaining validation of a new model of a heat exchanger from the results of experimental testing with simulations of an OTEC ocean thermal conversion power plant using a shell and tube heat exchanger model made of copper-tin alloy (Cu-Sn) with ammonia as the fluid. In order to achieve this goal, it is necessary to conduct investigations including: building a simulation flow diagram of the heat exchanger cycle and then assembling a prototype of the heat exchanger, analyzing and validating the results of simulation data processing and experimental investigation studies, and drawing conclusions from the results of the investigation.

4. RESEARCH MATERIALS AND METHODS

Chapter four is related to research materials and methods, which is a study in the research methodology section that discusses materials, methods, and research variables, prototype tool design, data collection techniques, and conclusions of the research flow diagram from a series of simulation and experimental studies.

4.1. Materials of research

In the experimental test, the focus of the research was a prototype of a new model of a Cu-Sn shell and tube heat exchanger. The shell was assembled from steel (Cu) and equipped with a tubing chamber for the working fluid ammonia made of copper alloy to produce good heat conductivity, which is assumed to be able to rotate the turbine. Meanwhile, the computer simulation research study used Aspen Plus and Computational Fluid Dynamics (CFD) applications.

4.2. Methods of Study

This experimental research was conducted in the energy conversion laboratory of Al-Azhar University by creating a prototype of a laboratory-scale heat exchanger to obtain experimental data in the form of inlet and outlet water temperatures from the heat exchanger area, seawater capacity, ammonia inlet and outlet temperatures, and mass flow rates, and then validated with the results of simulation research. CFD is a simulation method carried out in order to observe variations in the evaporator outlet temperature, condenser outlet temperature, warm water mass flow rate, and ammonia working fluid pressure. The evaporator condenser, pump, turbine, and electric generator are active components of the OTEC plant, which is a representation of a closed Rankine cycle [13]. Ammonia will form a saturated gas phase, which is expanded to drive the turbine. A simple ideal Rankine cycle calculates the work output of the power cycle and the cycle efficiency based on the design parameters [14].

4.3. Research Variables in the OTEC Research Simulation

The independent variables are based on simulation variation modeling. These include varying the seawater temperature leaving the evaporator, varying the seawater temperature leaving the condenser, varying the seawater mass flow rate, and varying the ammonia working fluid pressure. The dependent variable is the variable that changes after the independent variable is varied. These include varying the seawater temperature leaving the evaporator, varying the seawater temperature leaving the condenser, varying the seawater mass flow rate, and varying the ammonia working fluid pressure. Building a flow diagram of the cycle is the stage in the Aspen Plus simulation. The initial step is the flowsheet, which maps the entire system, flows, and unit operations that have been identified. The next step is to determine the chemical components of the thermodynamic process. The final step is to condition the temperature, pressure, and size. The heat exchanger simulation design results obtained from the ANSYS CFD simulation results for temperatures varying from 24°C to 28°C with 5-point variations.

Table 1. Boundary Conditions of Type A Heat Exchanger

Inf	Boundary Conditions	Type	Value
A.	inlet Ammonia	Mass flow rate	0,02 kg/s
	Inlet pressure - temperature	Inlet pressure-temperature	957.000 Pascal 8^0C
B	Ammonia outlet	Outlet pressure	0 Pa (gauge)
C	Water inlet	Mass flow rate	0,02 kg/s
	Inlet pressure	Inlet pressure	1.015 Pascal
D	Ammonia inlet temperature	Outlet temperaturepressure	30^0C 0 Pa (gauge)

Table 2. Boundary Conditions of Type B Heat

Inf	Boundary Conditions	Type	Value
A.	Inlet Ammonia	Mass flow rate	0,02 kg/s
	Preasure Inlet	Inlet pressure	957.000 Pascal
	Inlet Temperature	Temperature	8^0C
B	Outlet Amonia	Outlet Pressure	0 Pa (gauge)
C.	Inlet Water	Mass flow rate	0,02 kg/s
	Inlet pressure & temperature	Inlet pressure-temperature	1.015 Pascal 30^0C
D	Outlet 1 Amonia	Outlet Pressure	0 Pa (gauge)
	Outlet 2 Amonia	Outlet Pressure	Pa (gauge)

Tables 1 and 2 show that the Ansys CFD simulation process begins with importing geometry, followed by grid generation, and then defining boundary conditions. There are four boundary points: A, B, C, and boundary condition D. A represents the ammonia inlet boundary, B represents the ammonia working fluid outlet pressure, C determines the warm water inlet boundary, and the warm water inlet pressure and temperature. D determines the ammonia working fluid outlet. Table 3 presents the aspects and settings of a sign description that must be understood in the simulation process. The simulation is conducted from various perspectives, including the problem basis (solver model), viscosity basis (viscous model), materials, operating conditions, initiation, and residue monitoring.

Table 3. Computerization/Simulation aspects

Aspects	Arrangement
Basic Problem	Base pressure, three-dimensional, fluid condition: Steady
Viscosity Basics	Turbulent k-ε Standard Material: Air with constant density,
Operational Conditions	101325 Pa
Initiation	Inlet fluid velocity: (inlet residual velocity monitor 10^{-6})

4.4. Experimental Study of OTEC Work

The next concrete step is to create a heat exchanger prototype based on the best simulation results. The heat exchanger model is made of a copper-tin alloy (Cu-Sn). The design that is closest to the best of the two models is the heat exchanger prototype, Model A.

4.4.1. Production of heat exchangers

It has 32 tubing rod lines with 6 buffles assembled in a single pipe (tubing) circuit. The prototype design of a type A heat exchanger without an inlet hole in the middle is used as an experimental research access, which is a comparison with the type B heat exchanger design with an added hole in the middle of the HE unit. The production process for this research uses materials that are in accordance with the planning, design, and machine tools, according to existing standards.

4.4.2. Testing of shell and tube model heat exchangers at OTEC

After the shell and tube heat exchanger is finished being manufactured, the next step is the testing procedure and experimental data collection. The heat exchanger works with an evaporation system that occurs in some of the hot water that evaporates through the moving air flow, and the heat is lost to the atmosphere [15]. The components of the heat exchanger include: Pressure gauges on the inlet and outlet sides for both the working fluid and the seawater, seawater flowmeters, and tubing for the working fluid and seawater must be installed in the heat exchanger unit.

Figure 1. Seawater flowmeter and seawater inlet line.

The flowmeter is positioned in the heat exchanger unit, set at 200 l/h. The valve on the flowmeter control lever is positioned to only require 4 kg/s, as shown in Figure 2 below.

Figure 2. Observation of the pressure outlet from the ammonia condenser.

4.4.3. OTEC research data collection methods

Experimental testing, the data collection method takes data from nine criteria, including: time, ammonia inlet temperature, ammonia outlet temperature, seawater capacity, surface seawater inlet temperature, seawater outlet temperature from the evaporator, vapor pressure inlet from the condenser, vapor pressure exit from the condenser, mass flow rate, and ambient temperature. The initial method is carried out by running a CFD simulation, conducting an experimental study,, and then validating the results of both studies.

4.4.4. OTEC research flowchart.

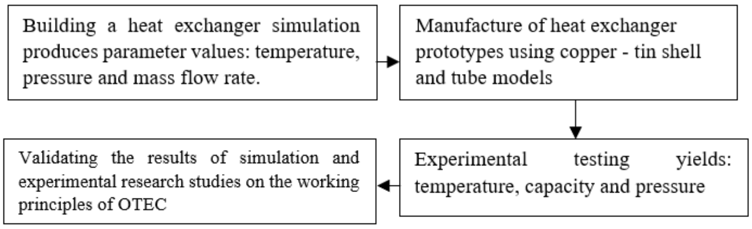

Figure 3. A brief sequence of the research flowchart

5. RESULTS AND DISCUSSION

This research initially used the ANSYS CFD computer simulation method, and the second stage used experimental methods. The OTEC system study parameters were a shell-and-tube heat exchanger model using Cu-Sn material, temperature, pressure, thermal conductivity, and basic technological principles. Two different models were developed to produce the best model for testing in the experimental study. Results for the heat exchanger/evaporator model A.

This model shows that there is no support void partition in the middle.

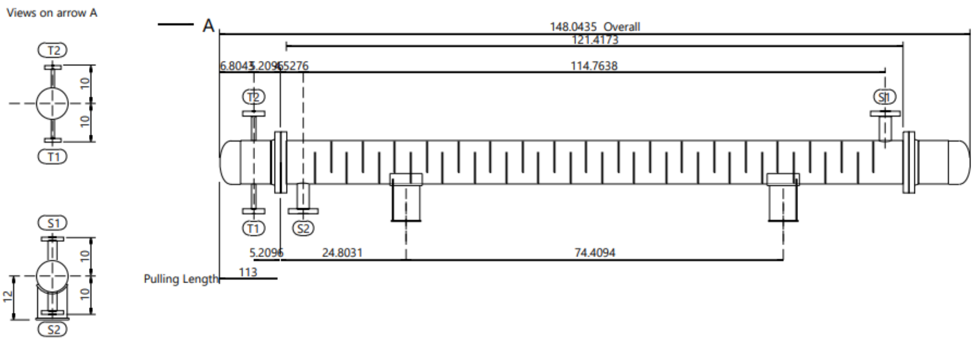

Figure 4. Heat exchanger/evaporator shell unit model

Results of heat exchanger / evaporator model B:

This model features a support void partition in the middle, which distinguishes it from Model A above.

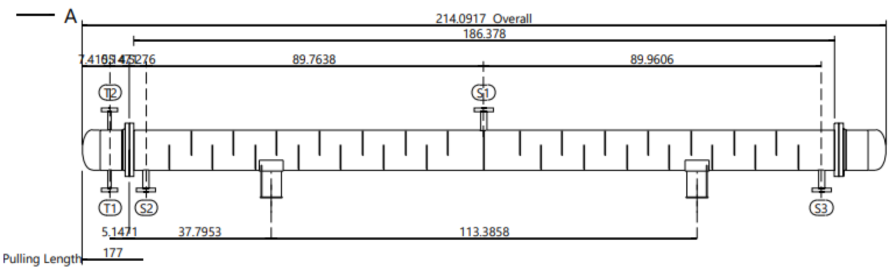

Figure 5. Model B heat exchanger/evaporator shell unit

5.1. Testing of Shell and Tube Heat Exchanger Simulation

Input parameters: The hot water entering the evaporator at sea level has a temperature of 30°C, which decreases to 28°C upon exiting the evaporator. The ammonia enters at 7.9°C and exits at 26°C. The results of the CFD simulation for model A are summarized in Table X below. (Note: The second row of Table X corresponds to the relevant chapter or subchapter and provides detailed values for each measured parameter.)

5.1.1. CFD Simulation of Temperature Contour Angle

The working fluid ammonia is at a temperature of 2.81 K (8°C) until the exit of the heat exchanger shell unit shows a temperature of 3.03 K (30°C). The CFD temperature starts with the entry of ammonia, which is at 2.81 K (8°C), and ends with the exit of the heat exchanger shell unit, showing a temperature of 3,010 K (30°C).

Table 4. Simulation Results of the temperature side of model A

Model	Parameter	Temperature Value (°K)
A	Inlet Temperatur Amonia	281.15 K
	Inlet Temperatur Air Pemanas	303.15 K
	Outlet Temperatur Amonia	281.15 K
	Outlet Temperatur Air Pemanas	301.15 K

In the evaporator system, the ammonia working fluid is at a temperature of 281 K (8℃) until the HE evaporator exits, showing a temperature value of 303 K (30℃). Meanwhile, for the heating water, the CFD temperature value begins with the entry of the heating water, which is at a temperature of 303.15 K (30℃) until the exit of the heat exchanger shell unit shows a temperature of 299.15 K (26.5℃).

Table 5. Simulation results of the temperature side of model B.

Model	Parameter	Temperature Value (°K)
B	Inlet Ammonia	281,15 K
	Inlet Hot Water	303,15 K
	Outlet Ammonia	299,45 K
	Outlet Hot Water	299,15 K

5.1.2. Ansys CFD Simulation Of Pressure Contour Angle

Shows the results of the distribution of pressure values in the pipe, starting with the entry of ammonia pressure at -3.15 Pa until it exits the heat exchanger shell with a pressure of 3.81 Pa. This occurs several times back and forth, not just a single turn, after which it exits the heat exchanger unit. ANSYS CFD simulation, when observed at the pressure contour angle, similar to the readings on the temperature contour angle, the distribution tends to increase as the pressure values in the component increase. The distribution value in the pressure pipe in the hot water begins with the entry of the pressure distribution at a temperature of 1.8 Pa until it exits the heat exchanger unit shell with a red mark indicating a temperature of 4.8 Pa.

Table 6. CFD simulation results of pressure contour angle of model A.

Model	Parameter	Pressure Value (Pa)
A	Inlet Ammonia Pressure	-3.15 Pa
	Heating Water Pressure Inlet	1,8 Pa
	Ammonia Pressure Outlet	3.81 Pa
	Heating Water Pressure Outlet	4,8 Pa

The pressure contour angle is nearly identical to the temperature contour angle. The closer the color is to the red distribution, the higher the pressure values in the heat exchanger shell component.

The figure shows the distribution of pressure values in the pipe, starting with the ammonia inlet at -1.832 Pa and ending with the exit of the heat exchanger shell unit at 3.81 Pa. This occurs several times, not just a single bend, after which the heat exchanger shell unit exits. The stress distribution values resulting from the simulation data are shown in Figure 5, model A below:

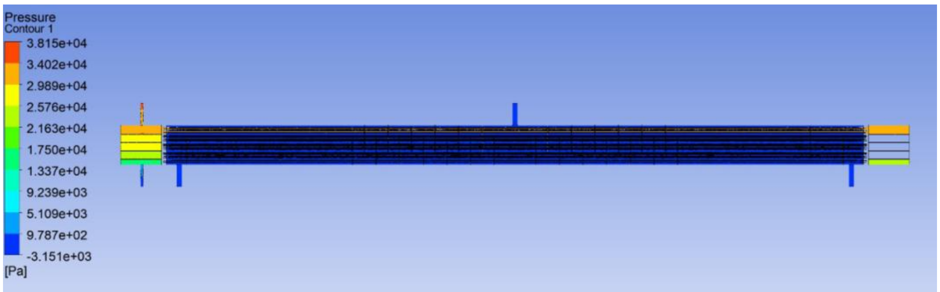

Figure 6. Pressure contour angle position in model A

The ANSYS CFD simulation, when observing the pressure contour angle, is similar to the temperature contour reading. The distribution tends to increase as the pressure values in the components increase. The distribution value in the hot water pressure pipe begins at 1,832 Pa and continues until the heat exchanger shell unit exits at 4.8 Pa.

Table 7. CFD Simulation Results of Pressure Side of Model B

Model	Parameter	Pressure Value (Pa)
B	Inlet Ammonia Pressure	-1.832 Pa
	Heating Water Pressure Inlet	1,8 Pa
	Ammonia Pressure Outlet	3.43 Pa
	Heating Water Pressure Outlet	4,8 Pa

The stress distribution value that occurs from the simulation work results from the data can be seen in Figure 4 model B below:

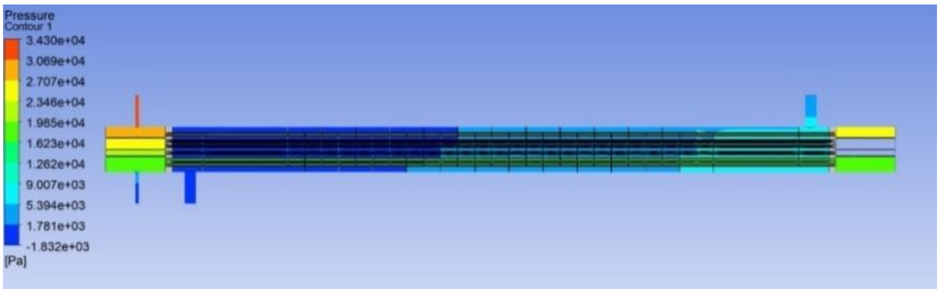

Figure 7. Pressure contour angle position of model B.

As seen in the image above, the closer the distribution toward red indicates higher pressure values in the heat exchanger shell unit component.

Compared to model A, model B does not yet exhibit significant pressure or temperature distribution values. Therefore, for experimental research, model A can be used as a reference for further experimental research.

5.1.3. Testing the Results of Hot Water Streamline Velocity in the Evaporator

The velocity streamline of hot water in the evaporator is shown in Figure 5 below, where the fluids are parallel but flow in opposite directions. This results in good heat transfer efficiency among existing heat exchanger types. However, in this experiment, there were two inlets because the water at the bottom was cold. around 50 °C entering the heat exchanger inlet position will meet the hot water coming out of the heat exchanger shell unit.

.

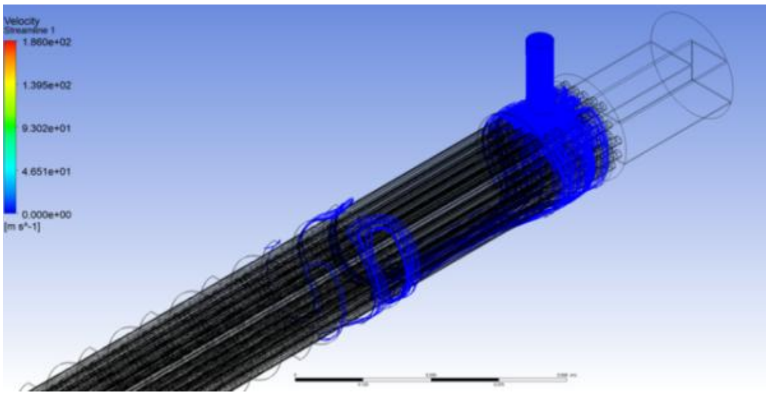

Gambar 8. *Velocity streamline* air panas pada evaporator HE tipe A

At a temperature of 300°C, warm water from the sea surface flows into the heat exchanger inlet through the shell side, and ammonia enters through the inlet tubing of the heat exchanger, turbulently passing through the installed baffle. The position of the fluid can be seen in Figure 6 below.

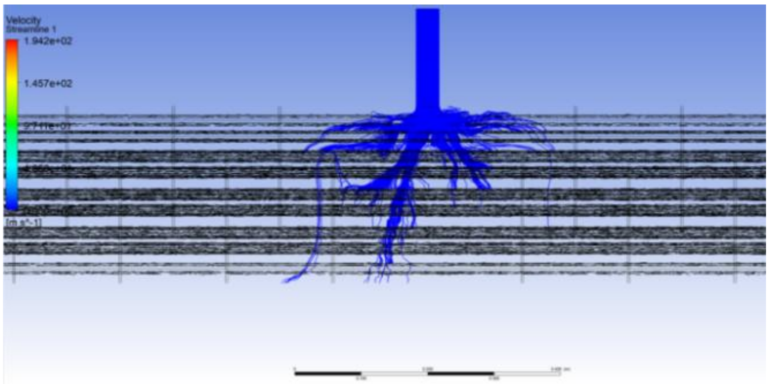

Figure 9. Results of the heat transfer efficiency of the hot water streamline velocity.

5.2. Experimental Testing Results of a Shell-and-Tube Heat Exchanger.

The experimental testing adopted seven work processes to generate accurate data. These work criteria include the working fluid outlet temperature, seawater capacity, seawater inlet temperature, seawater outlet temperature, condenser inlet vapor pressure, condenser outlet vapor pressure, mass flow rate, and ambient temperature..

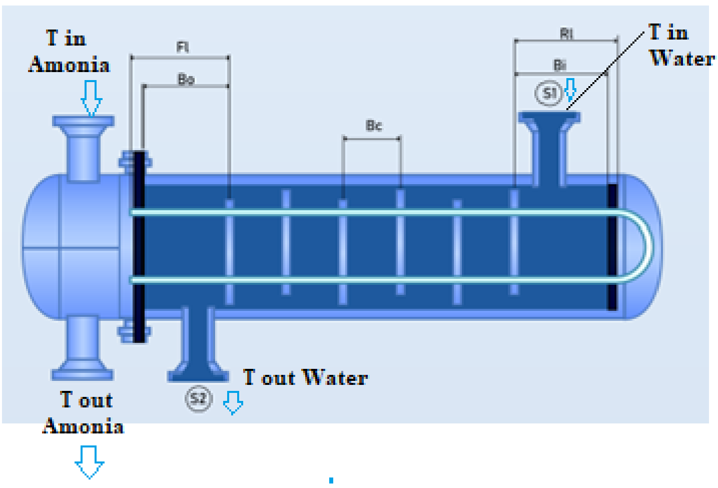

Figure 10. Heat exchanger unit for experimental data.

The effect of the copper tin alloy shell and tube heat exchanger system on Ocean Thermal Energy Conversion (OTEC) power plants can be seen in the following table.

Table 8. Test Results

T in Seawater (°C)	T out Seawater (°C)	Q Sea Water (l/h)	T in Ammonia (°C)	T out Ammonia (°C)	P in Ammonia (bar)	P out Ammonia (bar)
29.66	28.66	400	11.49	23.45	4.37	4.37
29.71	28.71	400	12.08	23.74	4.38	4.38
29.76	28.76	400	12.6	23.83	4.39	4.39
29.81	28.81	400	13.13	23.92	4.4	4.4
29.86	28.86	400	14.08	24.07	4.41	4.41
30	29	400	11.2	24	4.2	4.3

In this test, the sea surface water fluid entering (T_{in}) into the evaporator showed a temperature value of 29.10°C, and a phenomenon of temperature changes occurred at the ammonia inlet temperature of 11.49°C. And so on for 5 trials. From the graph trend of Figure 7, it can be seen that the seawater inlet temperature and the ammonia working fluid inlet temperature are functions of time, where the ammonia working fluid tends to experience an increase in temperature. When the working fluid temperature reaches 11,490 °C, and the seawater inlet temperature is stable at 29.66 ^{0}C

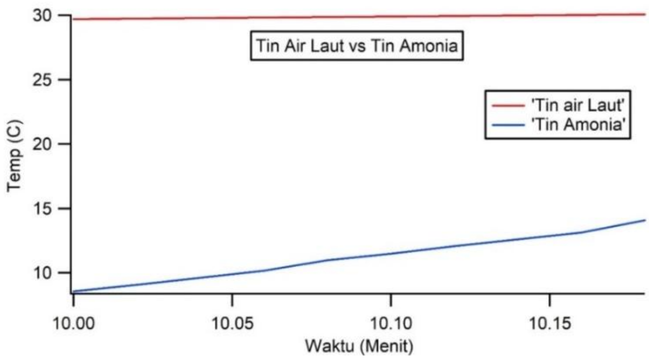

Figure 11. Seawater inlet temperature Vs Ammonia inlet temperature.

5.3. Mass Flowrate of Hot Water (ṁ).

The density of warm seawater fluid is ρ=1.206 kg/m^3. with a flow velocity of 0.877 m/s. then the mass flow rate (ṁ) becomes 0.114 kg/s.

5.4. Heat Capacity Released by Hot Water in the Evaporator (Q)

Take the specific heat of water by value $\mathbf{c_p} = (\mathbf{4200}\,\frac{\mathbf{J}}{\mathbf{kg}}\,°\text{C})$.

$$T_{h1} = 5{,}06,\ \ T_{h2} = 4{,}30,\ T_1 = 8{,}70, T_2 = 21{,}57$$

$$\text{Q} = 0.114\ {}^{\text{kg}}/_{\text{s}}\,(4200\ \frac{\text{kg}}{\text{J}}\,°\text{C})(0.72)°\text{C}$$

$$\text{Q} = 363\ \ \frac{\text{J}}{\text{s}} = 363 watt.$$

Table 9. Results of the calculation of heat released by hot water

ΔT_{eva} (°C)	A= $\pi/4$ d^2 (m²)	Qin Seawater 200 l/h (m^3/s)	V Velocity of Seawater (m/s)	Q_{eva} ṁ × $C_P \times \Delta T$ (watt)	Q_{cond} ṁ × C_P × ΔT (watt)	ΔT_{con} (°C)	($\dot{m}$) Mass flowrate (kg/s)
0.29	0.0001266	0,00011	0,877	133.852	363	0.72	0.114
0.272	0.0001266	0,00011	0,877	25.664	378	.72	0.114

6. CONCLUSION

The heat transfer coefficient value in the evaporator is 523 W/m^2 ^{0}C and the condenser is 524 W/m^2 ^{0}C, because in the ammonia working fluid tube space during the trial period, it must be maintained at 50 °C, based on a comparison of optimal performance results with other research experimental OTEC systems that have been published in the literature.

ACKNOWLEDGEMENT

Through this statement, the author would like to express his gratitude to his supervisor, Prof. Basuki Wirjosentono, Ph.D. and the entire team involved in completing this research. I would like to express my deepest gratitude to my colleagues involved in this research.

REFERENCES

[1] J. Langer, A. A. Cahyaningwidi, C. Chalkiadakis, J. Quist, O. Hoes, and K. Blok, "Plant siting and economic potential of ocean thermal energy conversion in Indonesia a novel GIS-based methodology," *Energy*, vol. 224, p. 120121, 2021, doi: 10.1016/j.energy.2021.120121.

[2] D. Vera, A. Baccioli, F. Jurado, and U. Desideri, "Modeling and optimization of an ocean thermal energy conversion system for remote islands electrification," *Renew. Energy*, vol. 162, pp. 1399–1414, Dec. 2020, doi: 10.1016/J.RENENE.2020.07.074.

[3] A. Hasan and I. Dincer, "An ocean thermal energy conversion based system for district cooling, ammonia and power production," *Int. J. Hydrogen Energy*, vol. 45, no. 32, pp. 15878–15887, Jun. 2020, doi: 10.1016/J.IJHYDENE.2020.03.173.

[4] J. Herrera, S. Sierra, and A. Ibeas, "Ocean thermal energy conversion and other uses of deep sea water: A review," *J. Mar. Sci. Eng.*, vol. 9, no. 4, Apr. 2021, doi: 10.3390/JMSE9040356.

[5] B. Wang, J. J. Klemeš, P. S. Varbanov, and M. Zeng, "An Extended Grid Diagram for Heat Exchanger Network Retrofit Considering Heat Exchanger Types," *Energies 2020, Vol. 13, Page 2656*, vol. 13, no. 10, p. 2656, May 2020, doi: 10.3390/EN13102656.

[6] Z. Wu, H. Feng, L. Chen, and Y. Ge, "Performance Optimization of a Condenser in Ocean Thermal Energy Conversion (OTEC) System Based on Constructal Theory and a Multi-Objective Genetic Algorithm," *Entropy*, vol. 22, no. 6, Jun. 2020, doi: 10.3390/E22060641.

[7] S. Zhou, X. Liu, K. Zhang, Q. Yue, Y. Bian, and S. Shen, "Evaluation of a novel ammonia-water based combined cooling, desalination and power system based on thermodynamic and exergoeconomic analyses," *Energy Convers. Manag.*, vol. 239, p. 114176, Jul. 2021, doi: 10.1016/J.ENCONMAN.2021.114176.

[8] C. Li, L. Pan, and Y. Wang, "Thermodynamic optimization of Rankine cycle using CO2-based binary zeotropic mixture for ocean thermal energy conversion," *Appl. Therm. Eng.*, vol. 178, no. December 2019, p. 115617, 2020, doi: 10.1016/j.applthermaleng.2020.115617.

[9] Y. Bian, J. Pan, Y. Liu, F. Zhang, Y. Yang, and H. Arima, "Performance analysis of a combined power and refrigeration cycle," *Energy Convers. Manag.*, vol. 185, pp. 259–270, Apr. 2019, doi: 10.1016/J.ENCONMAN.2019.01.072.

[10] J. Langer, J. Quist, and K. Blok, "Recent progress in the economics of ocean thermal energy conversion: Critical review and research agenda," *Renew. Sustain. Energy Rev.*, vol. 130, no. June, p. 109960, 2020, doi: 10.1016/j.rser.2020.109960.

[11] H. Feng, W. Chen, L. Chen, and W. Tang, “Power and efficiency optimizations of an irreversible regenerative organic Rankine cycle,” *Energy Convers. Manag.*, vol. 220, Sep. 2020, doi: 10.1016/J.ENCONMAN.2020.113079.

[12] K. Tamura, Y. Itsumi, H. Oyama, A. Okamoto, H. Arima, and Y. Ikegami, “Development of High Heat Transfer Titanium Sheet for Heat Exchanger,” *Proc. 13th World Conf. Titan.*, pp. 1825–1829, May 2016, doi: 10.1002/9781119296126.CH306.

[13] S. M. Abbas, H. D. S. Alhassany, D. Vera, and F. Jurado, “Review of enhancement for ocean thermal energy conversion system,” *J. Ocean Eng. Sci.*, no. xxxx, 2022, doi: 10.1016/j.joes.2022.03.008.

[14] O. Corigliano, A. Algieri, and P. Fragiacomo, “Turning Data Center Waste Heat into Energy: A Guide to Organic Rankine Cycle System Design and Performance Evaluation,” *Appl. Sci. 2024, Vol. 14, Page 6046*, vol. 14, no. 14, p. 6046, Jul. 2024, doi: 10.3390/APP14146046.

[15] F. Aulia, A. Syuhada, and R. Razali, “Analisis Eksperimental Perpindahan Panas Pada Menara Pendingin Tipe Plat Datar Bertingkat,” *J. Rekayasa Mesin*, vol. 15, no. 3, pp. 1621–1630, Dec. 2024, doi: 10.21776/JRM.V15I3.1821.